Supplementary Information: Microwave-Induced Ultralong-Range Charge Migration in a Rydberg Atom

Huihui Wang(王慧慧)[1,2], Yuechun Jiao(焦月春)[1,2], Jianming Zhao(赵建明)[1,2*], Liantuan Xiao(肖连团)[1,2], Suotang Jia(贾锁堂)[1,2]

[1]*State Key Laboratory of Quantum Optics and Quantum Optics Devices, Institute of Laser Spectroscopy, Shanxi University, Taiyuan, 030006, China;*

[2]*Collaborative Innovation Center of Extreme Optics, Shanxi University, Taiyuan, 030006, China*

I. PROPAGATION OF THE ELECTRON DENSITY

The Rydberg state $40S_{1/2}$ means a state with principle quantum number $n = 40$, quantum numbers for orbital angular momentum $l = 0$ and total angular momentum $J = 1/2$, respectively. Through this work we focus on Cs Rydberg atoms. The two involved states $40S_{1/2}$ and $40P_{1/2}$ with the same z-component of J ($m_J = 1/2$) will be written as $|40S_{\frac{1}{2},\frac{1}{2}}\rangle$ and $|40P_{\frac{1}{2},\frac{1}{2}}\rangle$, respectively. By solving the time-dependent Schrödinger equation we obtain the time propagation of the initial state $|\psi(t'=0)\rangle = \cos\gamma\,|40S_{1/2}\rangle + \sin\gamma e^{i\delta}\,|40P_{1/2}\rangle$ as

$$|\psi(t')\rangle = \cos\gamma e^{-iE_{40S_{1/2}}t'/\hbar}\,|40S_{\frac{1}{2},\frac{1}{2}}\rangle + \sin\gamma e^{i\delta-iE_{40P_{1/2}}t'/\hbar}\,|40P_{\frac{1}{2},\frac{1}{2}}\rangle\,, \tag{1}$$

where $E_{40S_{1/2}}$ and $E_{40P_{1/2}}$ are the eigenenergies of the two egenstates $|40S_{\frac{1}{2},\frac{1}{2}}\rangle$ and $|40P_{\frac{1}{2},\frac{1}{2}}\rangle$, respectively. In the representation of electron position $\mathbf{r}'$ and electron spin ξ', the wavefunction is $\psi(\mathbf{r}',\xi',t') = \langle\mathbf{r}',\xi'|\psi(t')\rangle$. The eigenfunctions of the two involved states can be factorized as

$$\begin{aligned}\langle\mathbf{r}',\xi'|40S_{\frac{1}{2},\frac{1}{2}}\rangle &= R_{40S_{1/2}}(r')\chi_{0\frac{1}{2}\frac{1}{2}}(\xi',\theta',\varphi'),\\ \langle\mathbf{r}',\xi'|40P_{\frac{1}{2},\frac{1}{2}}\rangle &= R_{40P_{1/2}}(r')\chi_{1\frac{1}{2}\frac{1}{2}}(\xi',\theta',\varphi').\end{aligned} \tag{2}$$

Here $R_{40S_{1/2}}(r)$ and $R_{40P_{1/2}}(r)$ are the corresponding radial wavefunctions. The radial wavefunction $R_{nlJ}(r)$ is obtained by the Alkali Rydberg Calculator (ARC) package codes as detailed in ref [1]. The effective one-electron potential includes the spin-orbit interaction term $\frac{\mathbf{L}\cdot\mathbf{S}}{137^2\times 2r^3}$ as implemented in the ARC codes. Consequently the effective potential and the radial wavefunctions depend on the quantum number J. Accordingly the radial probability densities $P(r) = r^2R_{nlJ}^2(r)$ of the $40S_{1/2}$ and $40P_{1/2}$ states are shown in Fig. S1.

The functions for electron spin ξ' and the two angles (θ',φ') are

$$\begin{aligned}\chi_{0\frac{1}{2}\frac{1}{2}}(\xi',\theta',\varphi') &= \alpha(\xi')Y_{00}(\theta',\varphi'),\\ \chi_{1\frac{1}{2}\frac{1}{2}}(\xi',\theta',\varphi') &= -\sqrt{\frac{1}{3}}\alpha(\xi')Y_{10}(\theta',\varphi') + \sqrt{\frac{2}{3}}\beta(\xi')Y_{11}(\theta',\varphi').\end{aligned} \tag{3}$$

Here $\alpha(\xi')$ and $\beta(\xi')$ are the spin wavefunctions for the states with spin-up and spin-down, respectively. And $Y_{lm}(\theta',\varphi')$ is the spherical harmonics. To simplify the notations, $R_{40S_{1/2}}(r)$ and $R_{40P_{1/2}}(r)$ will be written as $R_{40S}(r)$ and $R_{40P}(r)$, respectively.

The expression of the system wavefunction $\psi(\mathbf{r}',\xi',t') = \langle\mathbf{r}',\xi'|\psi(t')\rangle$ can be obtained from eqs. (1-3). The corresponding electron density $\rho(\mathbf{r},t')$ can be obtained by evaluating the mean value of the density operator

*Electronic address: zhaojm@sxu.edu.cn

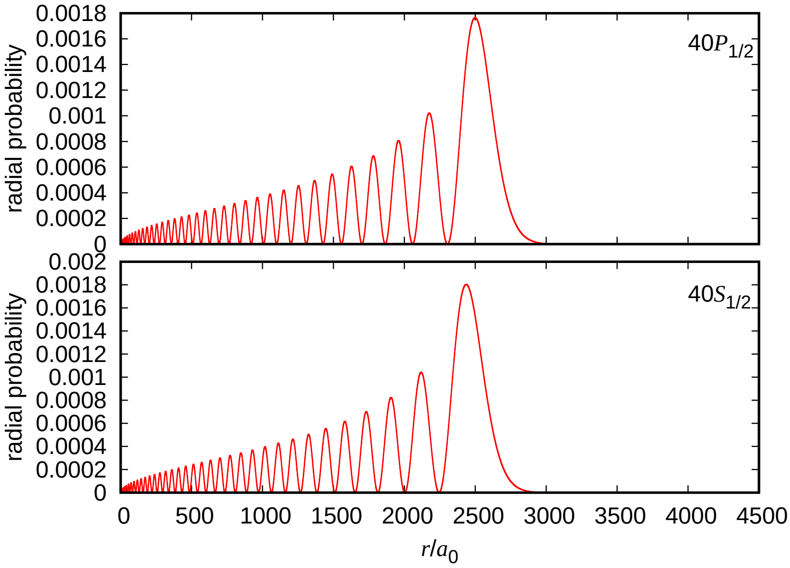

Figure S1: The radial probability density $P(r) = r^2 R^2_{nlJ}(r)$.

$$\begin{aligned}\rho(\mathbf{r},t') &= \langle\psi(t')|\delta(\mathbf{r}-\mathbf{r}')|\psi(t')\rangle \\ &\equiv \int \psi^*(\mathbf{r}',\xi',t')\delta(\mathbf{r}-\mathbf{r}')\psi(\mathbf{r}',\xi',t')d\mathbf{r}'d\xi' \\ &= \cos^2\gamma R^2_{40S}Y^2_{00} + \sin^2\gamma R^2_{40P}(\frac{1}{3}Y^2_{10} + \frac{2}{3}Y^2_{11}) \\ &- \sqrt{\frac{1}{3}}\sin 2\gamma\cos(\delta-\omega t')R_{40S}R_{40P}Y_{00}Y_{10},\end{aligned} \tag{4}$$

where $\omega = \frac{E_{40P_{1/2}} - E_{40S_{1/2}}}{\hbar} = 2\pi \times 63.6$ GHz.

The phase difference δ only defines the time reference. Observing $\rho(\mathbf{r},t')$ starting from different time will not change the essence of the charge migration phenomenon. For convenience we define $t' = \frac{\delta}{\omega}$ as the starting time for observing the density, namely a new time $t = t' - \frac{\delta}{\omega}$. The migrating part of the density is

$$\begin{aligned}\Delta\rho(\mathbf{r},t) &= \rho(\mathbf{r},t) - \langle\rho(\mathbf{r})\rangle_T \\ &= -\sqrt{\frac{1}{3}}\sin 2\gamma\cos(\omega t)R_{40S}R_{40P}Y_{00}Y_{10},\end{aligned} \tag{5}$$

where $\langle\rho(\mathbf{r})\rangle_T$ is the average density in one period $T = \frac{1}{63.6\text{ GHz}} = 15.7$ ps. Apparently $\langle\rho(\mathbf{r})\rangle_T$ is just the sum of the time-independent terms in Eq. (4).

Since the microwave is polarized along z-axis, the migrating part of the density $\Delta\rho(\mathbf{r},t)$ has cylindrical symmetry. It is then convenient to use the cylindrical coordinates (z,u,φ). The relations between the cylindrical coordinates, the spherical coordinates (r,θ,φ), and the cartesian coordinates (x,y,z) are

$$\begin{cases} z = r\cos\theta \\ u = r\sin\theta \\ \varphi = \varphi \end{cases}, \quad \begin{cases} x = u\cos\varphi \\ y = u\sin\varphi \\ z = z \end{cases}. \tag{6}$$

The migrating part of the density $\Delta\rho$ does not depend on φ. Figures S2a and S2b show the details of $\Delta\rho(z,u,t=0)$ and $\Delta\rho(z,u,t=\frac{T}{2})$, respectively. The net charge migration is apparently from $z<0$ to $z>0$ for $0<t<\frac{T}{2}$.

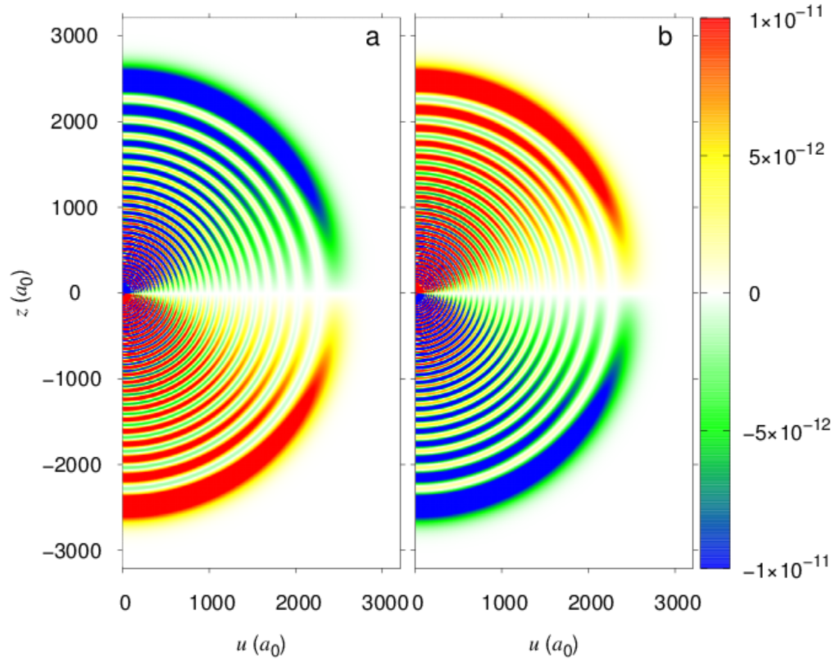

Figure S2: The migrating part of the density $\Delta\rho(z,u,\varphi,t)$ at a given time t for arbitrary φ in the cylindrical coordinates (z,u,φ). The unit of $\Delta\rho$ is a_0^{-3}. Panels A and B are for $t=0$ and $t=\frac{T}{2}$, respectively.

However there are also some small regions in which the charge migrates in the opposite direction. This is a consequence of the large number of nodes of the radial wavefunctions.

In the following we focus on the one-dimensional electron density $\Delta\rho(z,t)$ along z-axis

$$\Delta\rho(z,t)=\int_{-\infty}^{\infty}\int_{-\infty}^{\infty}\Delta\rho(\mathbf{r},t)dxdy=2\pi\int_{0}^{\infty}\Delta\rho(z,u,t)udu. \tag{7}$$

In the numerical calculations, we first get $\Delta\rho(z,u,t)$ in the cylindrical coordinates. Then we obtain $\Delta\rho(z,t)$ by integrating $\Delta\rho(z,u,t)$ over u. The one-dimensional densities $\Delta\rho(z,t)$ at different times are shown in Fig. S3.

II. THE ELECTRON FLUX DENSITY AND FLUX

The flux density can be obtained as the mean value of the flux operator

$$\begin{aligned}\mathbf{j}(\mathbf{r},t)&=\langle\psi(t)|\frac{\mathbf{P}}{2m}\delta(\mathbf{r}-\mathbf{r}')+\delta(\mathbf{r}-\mathbf{r}')\frac{\mathbf{P}}{2m}|\psi(t)\rangle\\&=\frac{\hbar}{4\sqrt{3}\pi m}\sin(2\gamma)\sin(\omega t)\\&\times[R_{40S}\nabla(R_{40P}Y_{10})-R_{40P}Y_{10}\nabla R_{40S}],\end{aligned} \tag{8}$$

where $\mathbf{P}=-i\hbar\nabla$ is the momentum operator. In the spherical coordinates, the flux density is

$$\mathbf{j}(\mathbf{r},t)=\hat{\mathbf{e}}_r j_r(\mathbf{r},t)+\hat{\mathbf{e}}_\theta j_\theta(\mathbf{r},t)+\hat{\mathbf{e}}_\varphi j_\varphi(\mathbf{r},t). \tag{9}$$

Apparently we have $j_\varphi(\mathbf{r},t)=0$. The other two components are

$$\begin{aligned}j_r(\mathbf{r},t)&=\frac{\hbar}{8\pi m}\sin(2\gamma)\sin(\omega t)\cos\theta[R_{40S}\frac{dR_{40P}}{dr}-R_{40P}\frac{dR_{40S}}{dr}],\\j_\theta(\mathbf{r},t)&=-\frac{\hbar}{8\pi m}\sin(2\gamma)\sin(\omega t)\frac{1}{r}R_{40S}R_{40P}\sin\theta.\end{aligned} \tag{10}$$

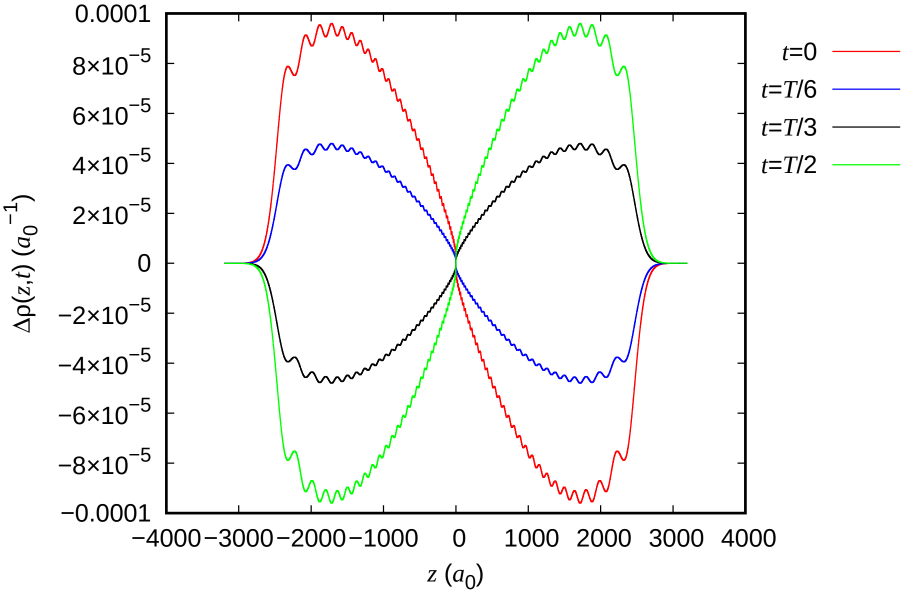

Figure S3: The migrating part of the density $\Delta\rho(z,t)$ at different time in units of a_0^{-1}.

The electron flux along z-axis F_z can be obtained by

$$F_z(z,t) = \int_{-\infty}^{\infty}\int_{-\infty}^{\infty} \mathbf{j}(\mathbf{r},t)\cdot\hat{\mathbf{e}}_z dxdy$$
$$= \frac{\hbar}{8\pi m}\sin(2\gamma)\sin(\omega t)\int_{-\infty}^{\infty}\int_{-\infty}^{\infty}[\cos^2\theta R_{40S}\frac{dR_{40P}}{dr} - \cos^2\theta R_{40P}\frac{dR_{40S}}{dr} + \frac{1}{r}\sin^2\theta R_{40S}R_{40P}]dxdy. \quad (11)$$

In principle we can carry out the above two-fold integration to get $F_z(z,t)$. However there is an alternative way to get the flux $F_z(z,t)$ according to the one-dimensional continuity equation

$$\frac{\partial F_z(z,t)}{\partial z} + \frac{\partial \rho(z,t)}{\partial t} = 0. \quad (12)$$

Accordingly the flux $F_z(z,t)$ can be evaluated by

$$F_z(z,t) = -\int_{-\infty}^{z}\frac{\partial\Delta\rho(z',t)}{\partial t}dz'. \quad (13)$$

Since we already have $\Delta\rho(z,t)$ at hand, the electron flux $F_z(z,t)$ is obtained by Eq. (13).

III. THE DIPOLE MOMENT AND THE MIGRATING CHARGE

The dipole moment of the system can be obtained by evaluating the mean value of the dipole operator

$$\boldsymbol{\mu}(t) = -\langle\psi(t)|e\mathbf{r}|\psi(t)\rangle\,. \quad (14)$$

The only nonzero component of $\boldsymbol{\mu}(t)$ is

$$\mu_z(t) = -\langle\psi(t)|ez|\psi(t)\rangle = -e\int_{-\infty}^{+\infty} z\Delta\rho(z,t)dz. \quad (15)$$

By numerical integration of eq.(15) we obtain $\mu_z(t) = \mu_z^{max}\cos(\omega t)$ with $\mu_z^{max} = 513.7\ ea_0 = 1305.7$ Debye.

The total migrating charge ΔQ_m can be obtained in terms of either the flux $F_z(z,t)$ or the density $\Delta\rho(z,t)$. The following four equivalent expressions all get the total charge which migrates from $z<0$ to $z>0$ (or the reverse) in a half period $\frac{T}{2}$:

$$
\begin{aligned}
\Delta Q_m &= -e\int_0^{\frac{T}{2}} F_z(z=0,t)dt \\
&= e\int_{\frac{T}{2}}^{T} F_z(z=0,t)dt \\
&= -e\int_{-\infty}^{0} [\Delta\rho(z,t=0)-\Delta\rho(z,t=\frac{T}{2})]dz \\
&= -e\int_{0}^{+\infty} [\Delta\rho(z,t=\frac{T}{2})-\Delta\rho(z,t=0)]dz \\
&= -0.35e.
\end{aligned}
\tag{16}
$$

IV. DETAILS FOR FEASIBLE EXPERIMENTAL REALIZATION

For the experiment, cesium atoms will be trapped in a magneto-optical trap (MOT) with a temperature of about 100 μK using laser cooling and trap technique. The MOT temperature can be further decreased to a few μK by an optical molasses and evaporation cooling technique. The ultracold Cs atoms are then loaded into a tightly focused optical tweeze to prepare a single atom and then optically pumped to the $|6S_{1/2}(F=4,m_F=4)\rangle$ Zeeman level with a circularly polarized laser. Rydberg excitation of the $|40S_{1/2}(m_J=1/2)\rangle$ state can be realized with a two-photon scheme as shown in Fig. S4a. Firstly a 852 nm laser with the σ^+ polarization drives the $|6S_{1/2}(F=4,m_F=4)\rangle$ to $|6P_{3/2}(F'=5,m_F=5)\rangle$ transition. Then a 510 nm laser with the σ^- polarization excites the $|6P_{3/2}(F'=5,m_F=5)\rangle$ state to the $|40S_{1/2}(m_J=1/2)\rangle$ state.

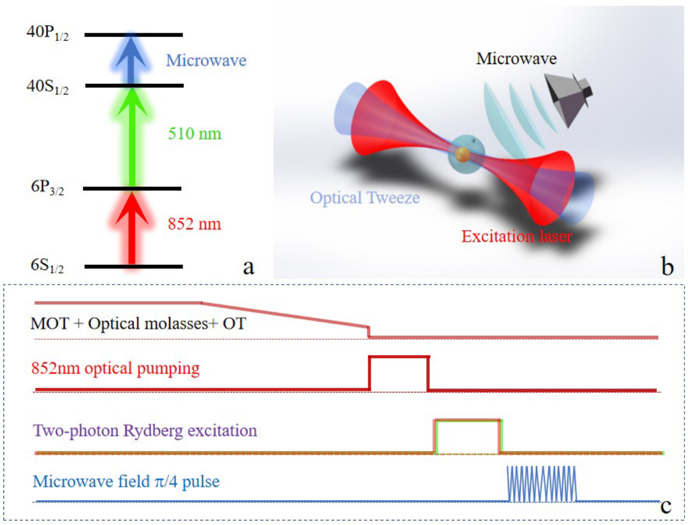

Figure S4: The scheme for the preparation of the initial state $|\psi(t'=0)\rangle$. a. Two-photon excitation to the Rydberg state $40S_{1/2}$ and partial transition from $40S_{1/2}$ to $40P_{1/2}$ by a microwave pulse. b. The experimental setup. The cesium atoms are first trapped in a MOT (not shown in here), then loaded into a optical tweeze (OT). c. The time sequence for loading and cooling, optical pumping, Rydberg excitation, and microwave transition.

After that, a linearly polarized (z-polarization) 63.6-GHz microwave field can be applied to couple the $|40S_{\frac{1}{2},\frac{1}{2}}\rangle$ and $|40P_{\frac{1}{2},\frac{1}{2}}\rangle$ states, which produces a superposition state of $|40S_{\frac{1}{2},\frac{1}{2}}\rangle$ and $|40P_{\frac{1}{2},\frac{1}{2}}\rangle$. The interaction between the microwave and a Cs atom is $-\boldsymbol{\mu}^{\mathrm{T}} \cdot \mathbf{E}$, where $\boldsymbol{\mu}^{\mathrm{T}}$ is the transition dipole moment and $\mathbf{E}$ is the amplitude of the microwave field. Since the field is z-polarized, we only need the z-component μ_z^{T}, which is -1305.2 Debye. By selecting appropriate microwave pulse parameters, the initial state can be prepared as $|\psi(t'=0)\rangle = \cos\gamma\, |40S_{\frac{1}{2},\frac{1}{2}}\rangle + \sin\gamma e^{i\delta}\, |40P_{\frac{1}{2},\frac{1}{2}}\rangle$. The details of the experimental setup and the time sequence of the applied external fields are shown in Figs. S4b and S4c, respectively. For the experimental condition with a field strength of 1.0 mV/cm and a pulse duration of 0.38 μs, $\gamma = \frac{\pi}{4}$ is reached which corresponds to equal population of the $40S_{1/2}$ and $40P_{1/2}$ states. This can be verified by the state-selective field ionization technique. The phase difference δ can not be determined. However the information we obtained is sufficient to unravel the essence of charge migration. Note the phenomenon of ultralong-range charge migration is more or less robust for different parameters δ and γ.

---

[1] Šibalić N, Pritchard J D, Weatherill K J and Adams C S 2017 *Comput. Phys. Commun.* **220** 319